Gaussian Beam Mode Analysis of Standing Waves Between Two Coupled Corrugated Horns

Neil Trappe, J. Anthony Murphy, *Member, IEEE*, Stafford Withington, *Member, IEEE*, and Willem Jellema

***Abstract*—In this paper we present the theoretical analysis of the effects of standing waves between coupled horn antennas that can occur in terahertz quasi-optical systems. In particular we illustrate the approach for the case of two coupled horn antennas as the distance between them is varied. The full mode matching scattering matrix approach is based on combining a standard waveguide mode description of the horn antenna and a quasi-optical Gaussian beam description of the free space propagation. Track is kept of both the backward and forward going components of the propagating fields. We compare theoretical predictions with actual experimental test results for a quasi-optical system operating at a frequency of 0.480 THz.**

***Index Terms*—Gaussian beam mode analysis, quasioptical systems, standing waves.**

I. Introduction

THE now standard theoretical framework for quasi-optical beam guide systems based on Gaussian beam mode analysis [1] can be successfully extended to include partial reflections and standing waves in THz optical systems fed by horn antennas. Propagation in the uniform waveguide and beamguide sections of the system can be accurately described in terms of the corresponding modes, with the effects of any discontinuities modeled using a mode matching approach [2]. By combining free space propagation using Gaussian Beam Mode Analysis [3] with waveguide modes in the horn, complete optical systems can be analyzed [4]. The horn is regarded as a combination of a large number of waveguide segments in succession, which match the horn profile. At each junction power is scattered between adjacent modes. In the modal view of propagation waveguide modes are transformed at the horn aperture to free space Gaussian modes that subsequently propagate through the optics. Laguerre-Gaussian modes are most convenient for free space propagation when the horn feeds possess a high degree of cylindrical symmetry. The techniques available within Gaussian Beam Mode theory [3] to describe beam guide systems include effects such as truncation [5].

Manuscript received April 29, 2003; revised July 8, 2004. This work was supported in part by Enterprise Ireland (Prodex), the Science Foundation Ireland (SFI), and in part by the National University of Ireland, Maynooth.

N. Trappe and J. A. Murphy are with the National University of Ireland, Maynooth, Ireland.

S. Withington is with the Cavendish Laboratory, Cambridge CB3 0HE, U.K.

W. Jellema is with the Space Research Organisation of the Netherlands (SRON), 9700AV Groningen, The Netherlands.

Digital Object Identifier 10.1109/TAP.2005.846453

II. Theory

The characteristics of a section of the horn-quasi-optical system are represented by a scattering matrix that describes the redistribution of power between adjacent modes (equivalent to waveguide modes or free space modes). The mode coefficients of the forward and backward propagating modes at the input and output planes of any subsection or even the optical system as a whole are related through the usual scattering matrix relationships, as for example in [2]. Each part of the system is analyzed separately to determine the appropriate scattering matrix for the subsection and these are then cascaded, where the cascaded matrix elements are of the usual form, again for example as in [2]. A horn antenna can be regarded as a tapered waveguide with nonconstant diameter along the axis of propagation.

At the horn aperture transverse electric (TE) and transverse magnetic (TM) waveguide modes are transformed to free space modes (Gaussian Beam modes). The transformation matrix requires the computation of the appropriate overlap integrals. The transverse electric field $\mathbf{E}_{\text{total}}$ at the mouth of the horn can be written as a linear sum of TE and TM modal fields. If one is considering conical horns (both smooth walled and corrugated), fed with a single TE_{11} mode polarized in the x direction, then the waveguide segments are cylindrical and the appropriate TE and TM modes $\boldsymbol{e}^{\text{TE}}$ and $\boldsymbol{e}^{\text{TM}}$ can be written in the form [4]

$$\mathbf{e}_{1l}^{\text{TE}} = \frac{J_0\left(\frac{p'_{1l}r}{a}\right)\mathbf{i} + J_2\left(\frac{p'_{1l}r}{a}\right)[\cos 2\phi\mathbf{i} + \cos 2\phi\mathbf{j}]}{\sqrt{2\pi a^2\left(J_1\left(\frac{p'_{1l}r}{a}\right)^2 - J_2\left(\frac{p'_{1l}r}{a}\right)^2\right)}}$$

$$\mathbf{e}_{1l}^{\text{TM}} = \frac{J_0\left(\frac{p_{1l}r}{a}\right)\mathbf{i} - J_2\left(\frac{p_{1l}r}{a}\right)[\cos 2\phi\mathbf{i} + \cos 2\phi\mathbf{j}]}{\sqrt{2\pi a^2\left(J_2\left(\frac{p_{1l}r}{a}\right)^2\right)}}, \quad (1)$$

where p_{1l} in (1) represents the lth zero of $J_1(z)$, and p'_{1l} represents the lth zero of $J'_1(z)$. The modes are normalized in such a way as to make the integral $\int_A |\mathbf{e}_l^{\text{TE/TM}}|^2 2\pi r dr$ equal to unity. For free space coupling to a conical horn it is most appropriate to employ the Associated Laguerre–Gaussian set because of the cylindrical symmetry of the system. For a wave travelling in the positive z direction these have a general form given by (2) [3], where α is an integer representing the degree of the Laguerre polynomial. W and R have their usual significance and $\arctan(\pi W^2/\lambda R)$ is the zero order phase slippage [3]. The waveguide modes of a conical horn will clearly couple only to

free space Associated Laguerre Gaussian modes of degree 0 and 2.

$$\begin{aligned}
&\begin{pmatrix}\Psi_n^{\alpha,\cos}(r,\phi)\\ \Psi_n^{\alpha,\sin}(r,\phi)\end{pmatrix}\\
&\quad=\Psi(r,\phi)_n^{\alpha}\exp\left(-ikz+i(2n+\alpha+1)\right.\\
&\qquad\left.\times\arctan\left(\frac{\pi W^2}{\lambda R}\right)\right)\begin{pmatrix}\cos(\alpha\phi)\\ \sin(\alpha\phi)\end{pmatrix}\\
&\quad=\sqrt{\frac{2(2-\delta_{0n})n!}{\pi W^2(n+\alpha)!}}\left(2\frac{r^2}{W^2}\right)^{\frac{\alpha}{2}}L_n^{\alpha}\left(2\frac{r^2}{W^2}\right)\\
&\qquad\times\exp\left(-\frac{r^2}{W^2}\right)\exp\left(-ik\left[\frac{r^2}{2R}\right]\right)\\
&\qquad\times\exp\left(-ikz+i\left(2n+\alpha+1\right)\times\arctan\left(\frac{\pi W^2}{\lambda R}\right)\right)\\
&\qquad\times\begin{pmatrix}\cos(\alpha\phi)\\ \sin(\alpha\phi)\end{pmatrix}. \qquad (2)
\end{aligned}$$

Each waveguide mode field is transformed to the corresponding free space mode using

$$\mathbf{e}_m^G=\sum_n T_{nm}^0\Psi_n^0\mathbf{i}+T_{nm}^2\Psi_n^2[\cos 2\phi\mathbf{i}+\sin 2\phi\mathbf{j}] \qquad (3)$$

where T_{nm}^0 and T_{nm}^2 are given by

$$T_{nm}^0=\int_A\left(\Psi_n^0\bar{\mathbf{i}}\right)^*.\left(\mathbf{e}_m^G\right)rdrd\phi \qquad (4a)$$

$$T_{nm}^2=\int_A\left(\Psi_n^2\bar{\mathbf{n}}\right)^*.\left(\mathbf{e}_m^G\right)rdrd\phi \qquad (4b)$$

where $\mathbf{n}$ represents the unit vector $\mathbf{n}=\cos 2\phi\mathbf{i}+\sin 2\phi\mathbf{j}$. The overall horn aperture field $\boldsymbol{e}_{\text{total}}$ is given by

$$\mathbf{e}_{\text{total}}=\sum_n B_n^0\Psi_n^0\mathbf{i}+B_n^2\Psi_n^2[\cos 2\phi\mathbf{i}+\sin 2\phi\mathbf{j}]. \qquad (5)$$

Clearly using (5), the coefficients B^0 and B^2 for the Laguerre modes of degree 0 and 2 can be written as

$$B_m^0=\sum_m T_{nm}^0A_n \quad\text{and}\quad B_m^2=\sum_n T_{nm}^2A_n. \qquad (6)$$

Incorporating this transformation to free space into the modal matching technique, described in (4), the matrix will have the form

$$[S]=\begin{bmatrix}S_{11}&S_{12}\\ S_{21}&S_{22}\end{bmatrix}=\begin{bmatrix}0&T^+\\ T&0\end{bmatrix} \qquad (7)$$

where T^+ represents the conjugate transpose of T. The transformation matrix $[T]$ can be regarded as the $[S_{21}]$ matrix component of a scattering matrix $[S]$ that transforms the waveguide to beam guide modal descriptions of the propagating fields at the plane of the horn aperture. As reversing the direction from free space to waveguide the $[S_{12}]=[S_{21}]^{T+}$, where T^+ represents a conjugate transpose. For a horn whose aperture is wide compared to the wavelength of the incident radiation (several wavelengths wide) it can be assumed that there is no appreciable reflection of the waveguide modes at the aperture. This implies that $[S_{11}]=[0]$, as only the highest order modes, which contribute little to the beam, will have a guide impedance appreciably different from that of free space. Also, free space radiation propagating in the negative direction toward the horn and which misses the horn mouth is not reflected again and is considered lost, thus $[S_{22}]=[0]$. The cross section of the reflected beam that overlaps with the horn will be coupled to the waveguide modes by the $[S_{12}]$ matrix.

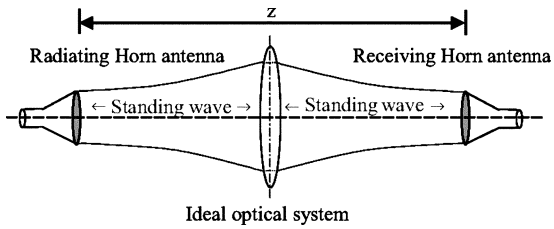

Fig. 1. Two corrugated horns matched by an ideal lens. The standing wave profile is observed by measuring the transmitted power in the waveguide of the receiving horn (S_{21} for the system).

In certain situations when the waveguide is only a few wavelengths across it is possible to include the effect of the reflection at the horn aperture by modeling the final step to free space as a waveguide step to a large waveguide. This approach is more computationally intensive as the number of waveguide modes required to describe the field increases, since the mode set is defined by a guide with a diameter equal to the larger guide.

III. Examples

We now apply the above theory to two specific examples. In the first case, an ideal optical system is placed between the horns. In effect the phase curvature of the first horn field is transformed to fit the phase curvature of the second horn and the free space fundamental mode component of the two beams are perfectly matched. This setup is illustrated in Fig. 1, where we assume the phase transformer is a perfect lossless thin dielectric lens. As the aperture separation is increased, the focal length of the lens is also adjusted to correctly transform the phase curvature. This simple model is representative of heterodyne receivers where a local oscillator (LO) source is matched to the detector horn via an optical system and so this model has important implications for system design.

In a second example, we consider the case where the two horns face each other with no intermediate optics. As the distance z is incremented the radiated power from the first horn is not focused to the aperture of the second horn, but spreads diffractively. This second example is relevant for near field measurements of horn antenna patterns using a scanning horn, where a standing wave may be set up on axis between the horns. Additionally, standing wave effects were explored experimentally in a test setup. We compare the results obtained with the model predictions.

Case A: Quasi-Optically Coupled Horns: In this example the modal matching technique is used to predict the overall transmission and reflection properties [4] of the setup illustrated in Fig. 1. To keep track of the free space beam mode parameters,

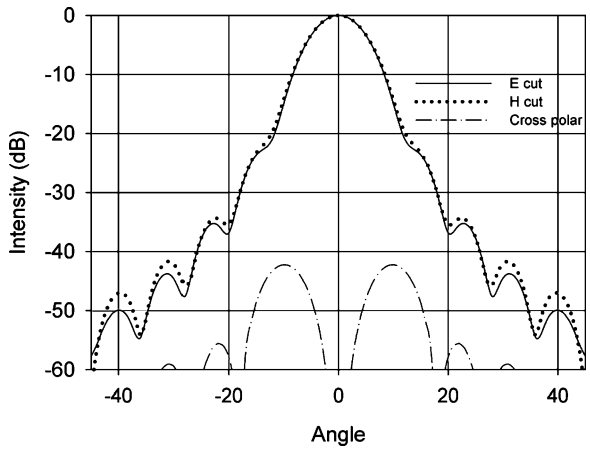

Fig. 2. Theoretical far-field plots in the E-plane and H-plane of the horns. Also shown is the cross-polar power in the D plane.

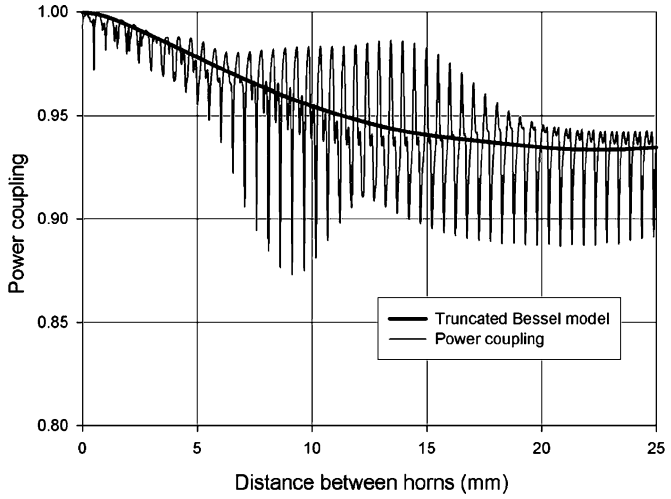

Fig. 3. Power coupling between two corrugated horns as the distance between the apertures is incremented from the apertures touching to a distance of 25 mm. Also shown is the average power coupling between the horns with no reflections included.

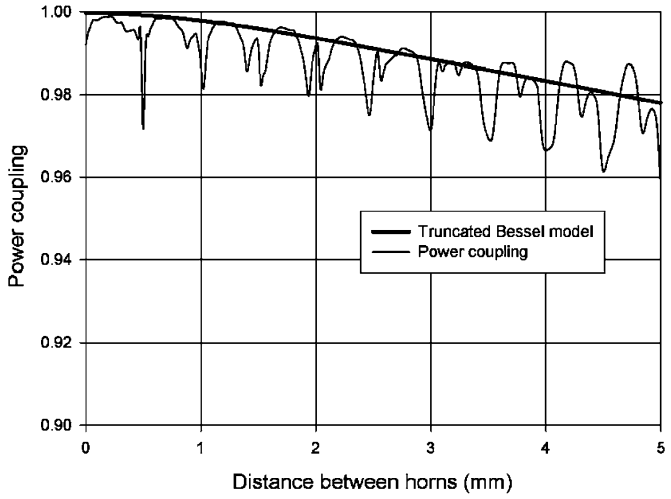

Fig. 4. The power coupling between two corrugated horns as the distance is varied from 0 to 5 mm, highlighting the cavity resonances separated by $\lambda/2$ distances. Also shown (thick line) is the power coupling between the horns calculated using a simple truncated Bessel model.

the classical ABCD matrix technique is used [6]. What is of interest is the amount of power coupled between the waveguide sections of each horn. Thus, to observe the transmission properties of the entire optical system between the two waveguides, the corresponding total cascaded S_{21} matrix is computed as a function of the distance z between the horns. The waveguide radii are limited to allow only the TE_{11} to propagate there, as would be the normal case. For efficiency we limit the number of modes to 20 waveguide modes (10 TE and 10 TM) within the horn structure and 20 freespace Gaussian modes (10 Laguerre of degree 0 and 10 modes of degree 2).

The wavelength chosen for the analysis is $\lambda = 1\,\mathrm{mm}$, the two horns are of the same design with a slant length of 40 mm, an aperture radius of 4 mm and 3 corrugations per wavelength. This theoretical horn produces good symmetry between the E and H plane. A theoretical far-field pattern to illustrate the symmetric E and H cuts is shown in Fig. 2. The low cross-polar levels associated with this particular horn design indicate that it is of an optimal design.

Fig. 3 illustrates the standing wave profile calculated as the distance between the two horns is incremented in steps of $\lambda/50$ between $z = 0$ to 25 mm. This is the power coupling $P_{21}|S_{21}(\mathrm{TE}_{11} \rightarrow \mathrm{TE}_{11})|^2$ plotted as a function of z, the distance between the two apertures. Physically this corresponds to the power reaching the waveguide section of the receiving horn and carried by the fundamental TE_{11} mode, the only mode that can propagate in the waveguide there.

As can be seen in Fig. 3 the estimated power coupling P_{21} between the two horns appears to have standing wave features. In effect, this optical setup acts like as a lossy cavity with some power trapped within the system. It is noticable in Fig. 4, where the coupling is shown when the horns are only seperated by distances up to 5 mm, that the features are seperated by increments in z of $\lambda/2$, illustrating cavity behavior in the system.

Also shown in Fig. 3 is the calculated power coupling between the two horns, when the aperture fields are approximated by the usual truncated Bessel function of order zero with the appropriate phase curvature term to represent the slant length of the horns ($E = J_0(2.405r/a)\exp(-jkr^2/2L)$, where a is the radius of the guide, L is the slant length [7]). Using a technique, described in detail in [8], the mode coefficients are calculated for each horn (A_m, B_m) and the horn to horn power coupling η can be calculated for this ideal optical system using

$$\eta = \left| \sum_m (A_m B_m^*) \exp\left(j(2m+1)\Delta\phi_{00}\right) \right|^2, \qquad (8)$$

where $\Delta\phi_{00}$ the refers to the total phase slippage between the horn apertures. It can be seen from Fig. 3 that the overall power coupling calculated using the full modal description of the horns matches closely the coupling calculated using the more basic description of the system with reflection not included.

The assumption made in the results shown in Figs. 3 and 4 is that all the radiation reaching the waveguide of the horns is transmitted and no power is reflected at the waveguide of the horn. In real systems of course, there may be a detection device

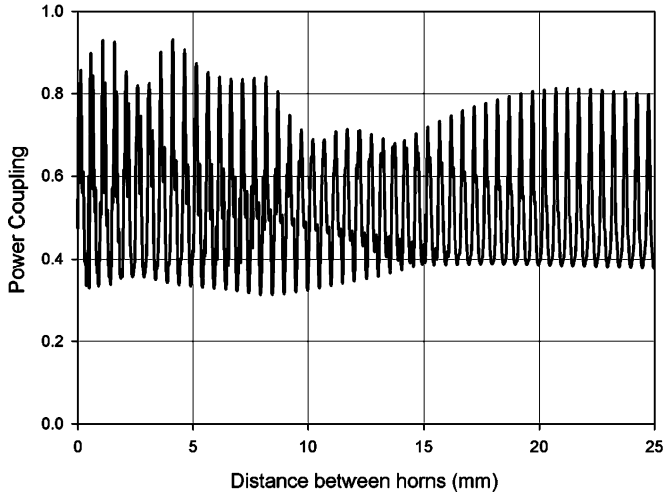

Fig. 5. Power coupling between two corrugated horns as the distance is varied from 0 to 25 mm, including an extra reflection at the waveguide in the horn to represent reflections at the some waveguide device.

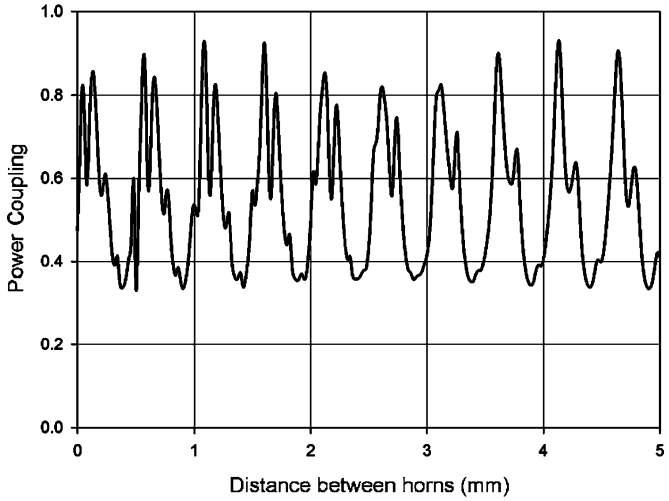

Fig. 6. Power coupling between two corrugated horns as the distance is varied from 0 to 5 mm, including an extra reflection at the waveguide in the horn to represent reflections at some waveguide device.

placed in the receiver waveguide, and this might not absorb all incident radiation but reflect a portion of the power back out into the horn. A similar situation may occur in the source due to a multiplier diode, for example. To include this effect in the computational model we approximate the detection or source device mismatch by a simple partially reflecting sheet in the waveguide which have certain reflection and transmission coefficients. In this simple model some of the power carried by the fundamental TE_{11} mode is reflected back to the corrugated horn while a fraction is also transmitted down the waveguide (actually representing detected power by the detection device or radiated power by the source device).

The transmission and reflection coefficients r and t at these equivalent partially reflecting plane surfaces relate how much of the incident beam is transmitted and how much is reflected. These coefficients are related to the reflectivity R and the transmissivity T of the semi-reflecting sheets through the following:

$$R = |r|^2 \quad T = |t|^2. \tag{9}$$

When the system is taken to be lossless the reflectivity and transmissivity are related by [1]

$$R + T = 1. \tag{10}$$

The semi-reflecting sheet is included in the modematching technique using the equation

$$\begin{vmatrix} S_{11} & S_{12} \\ S_{21} & S_{22} \end{vmatrix} = \begin{vmatrix} r & t \\ t & r \end{vmatrix}. \tag{11}$$

The effects of including the extra reflection in the waveguide of the horn is illustrated in Fig. 5 and 6 over the same ranges of between 5 and 25 mm between the horn apertures. In this particular example the reflectivity R is set to 20%. The power coupling between the horns has fallen as all the power cannot be absorbed and the profile of the power coupling has changed due to an extra reflection being included. The exact effect any real waveguide device has on the incident beam is more difficult to model accurately and what we have presented here is of course a simplified alternative.

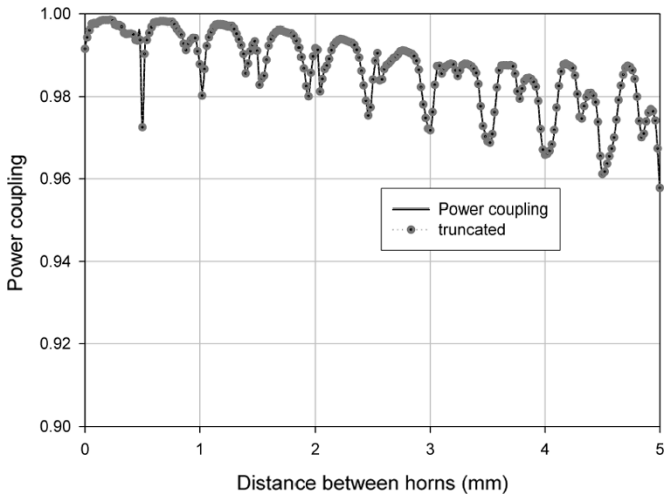

Fig. 7. Power coupling between two corrugated horns as the distance is varied from 0 to 5 mm, with 4 W truncation (dashed line) included.

In the analysis presented thus far the ideal optical system transmits all radiation between the two horns with no loss. Clearly, in a real optical system the higher order freespace modes are truncated by finite optical components (high spatial frequency filtering). Any losses in the optics might clearly reduce the cavity effects and therefore in order to describe a more physically meaningful system, the number of modes allowed to propagate between the horns is limited by introducing beam truncation. In Fig. 1 this can be modeled by introducing a circular aperture at the lens which automatically limits the higher order modes (and throughtput) in the system. Fig. 7 compares the power coupling of the system when a truncating aperture is included with a diameter of $4W$, where W is the local beam width parameter at the lens. It is noticable, that when a truncating aperture is included, the cavity effects are still evident indicating lower order modes are responsible for these cavity effects.

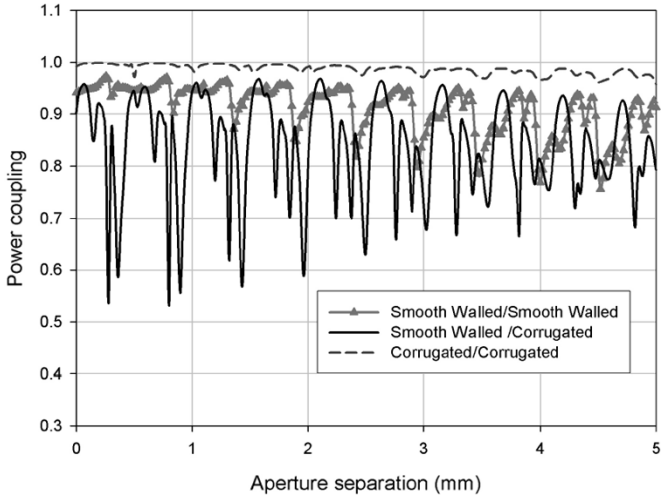

Fig. 8. Comparison of horn to horn coupling calculated using different horn geometries.

Additionally, we analyze the power coupling profile that occurs between two different horns, matched by an intermediate optical system. Fig. 8 illustrates some examples. In the first case a corrugated horn is coupled to a smooth walled horn having the same aperture radius and slant length. The resonances now occur at different inter-horn distances indicating that the geometry of the horn is important. Also, we calculate the power coupling between two smooth walled horns and it is noticeable that again the profile structure is different. In each case the resonances are still separated by a distance z equal to $n\lambda/2$. This clearly indicates the power coupling for each horn combination in this optical setup is dependent on the individual horns used. The lower average coupling between the two smooth walled horns reflects the fact that the fields are less Gaussian.

Case B: Coupled Horns With No Intermediate Optics: We now consider a second case where two horns are not matched by coupling optics, but rather power is coupled directly via free space propagation to the second horn. This example was also investigated experimentally. We could thus compare the model predictions with experimental results. The test setup is a near field phase locked detection system operating at 480 GHz. The details of the system are described in another paper [9]. Two conical corrugated horns (whose geometry is well known) are initially placed together aperture to aperture. Experimentally the distance z between the horns is incremented in step sizes of the order of $\lambda/20$ and a measurement is recorded as the receiving horn travels on an accurate moving stage. The design wavelength of the corrugated horn is 0.625 mm (480 GHz) and the horn aperture has a radius of 2.5 mm and has a slant length of 15.4 mm. The power coupling between the horns is shown in Fig. 9 over an aperture separation ranging from 0 to 70 mm.

The same method of analysis as used above in case A is implemented to predict the overall transmission and reflection properties of the system. In this case as no lens is included between the horns, the power coupling levels are lower and as the distance z is increased the transmitted field expands transversely to the propagation axis and so only part of this field can couple to the receiving horn. A partially reflecting sheet is again used to model the reflections due to the mixer at the waveguide section of the horn, with $R = 50\%$.

Fig. 9(a) shows the measured and predicted power coupling between the two horns as a function of horn separation over a range of 0 to 14 mm, while Fig. 9(b) illustrates the coupling over the complete 70 mm range, the maximum possible for the axial translation stage in the measurement setup. As can be seen in Fig. 9(a) and (b) the estimated power coupling P_{21} between the two horns appears to have significant high Q cavity features in contrast to the previous example, particularly when the distance between the horns is small (0 to 5 mm). As the distance between the apertures increases the power coupling becomes more regular and quasisinusoidal.

In the range of 4 to 10 mm, the model predicts the experimental pattern with high accuracy. When the separation of the horns is less than 4 mm, the amplitudes of the simulated standing wave pattern appear to be too large although the erratic behavior of its form has similar characteristics to the experimental result. At such close distances to the horn apertures, of course, evanescent and nonparaxial components of the fields will become important and the simple paraxial assumptions in the free space mode model will not be adequate to predict exactly the behavior of such a high Q system.

Similarly although over the horn separation range of 10 to 30 mm the model underestimates the amplitudes of the standing wave pattern, as seen in Fig. 9(a) and (b), nevertheless the form of the standing waves and the locations of the nodes and antinodes are accurately reproduced. The mixer in the waveguide at the throat of the horn is treated in the model, as a simple dielectric reflector having a constant reflectivity, which is clearly an approximation, in particular as there will be some dependence of the reflectivity on the amount of incident power.

The model therefore reproduces well many of the important features of the standing wave behavior of the experimental system and the approach can clearly be used to develop strategies for reducing such effects.

Indeed, the average power coupling between the horns shows very good agreement between the experimental and theoretical results over the full 70 mm range, as illustrated in Fig. 9(b). Although certain detailed features of the experimental standing wave profile are not reproduced exactly by the model the overall characteristic decay in the coupling is predicted very precisely.

If one examines the scattering matrices which describe the horn to horn coupling one finds that a small amount of power is scattered from the TE_{11} mode to higher order modes as the radiation propagates through the horn. These modes are only weakly coupled to the fundamental TE_{11} mode and so become trapped between the two horns since they are effectively reflected at the second horn before reaching the throat. If the distance between the two horns is such that the return trip is an integer number of wavelengths resonance effects are seen. In fact, the effect is dominated by multiple reflections of the TM_{11} mode.

As a further verification of the model, Fig. 10 shows the horn power coupling calculated using a simple truncated Bessel model for the corrugated horn compared to the full model description used above. The overall power coupling, as the aperture separation is increased, calculated using the two different techniques is seen to agree and the power coupling falls off at the same rate with increasing distance.

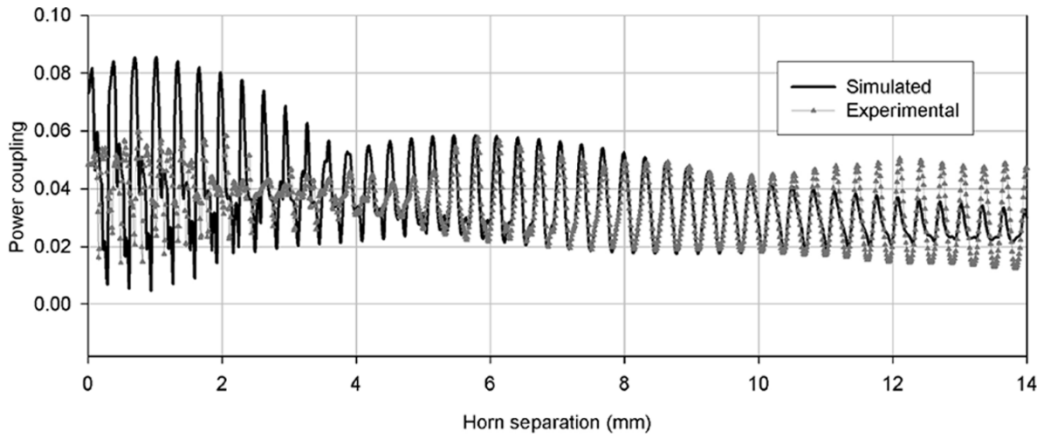

(a)

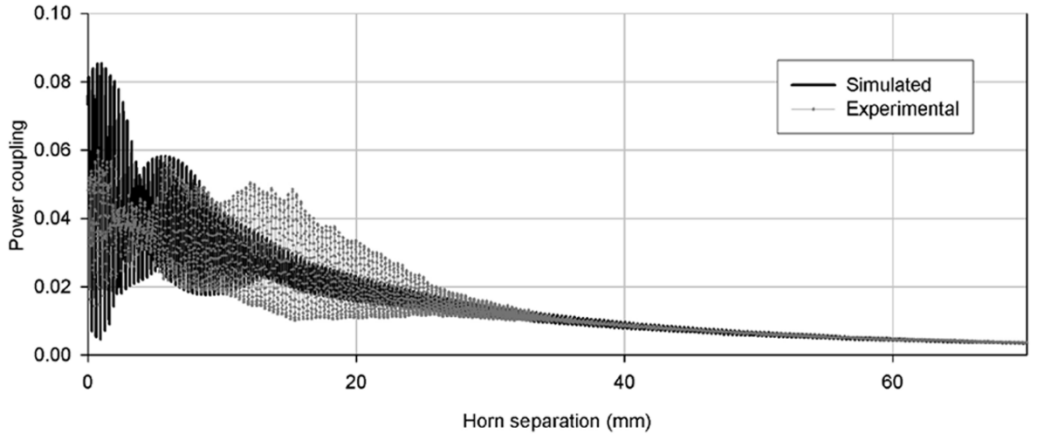

(b)

Fig. 9. Experimental power coupling compared to the analytical predictions for two aperture separation ranges (a) illustrates the comparison over a 14 mm range and (b) over a 70 mm range.

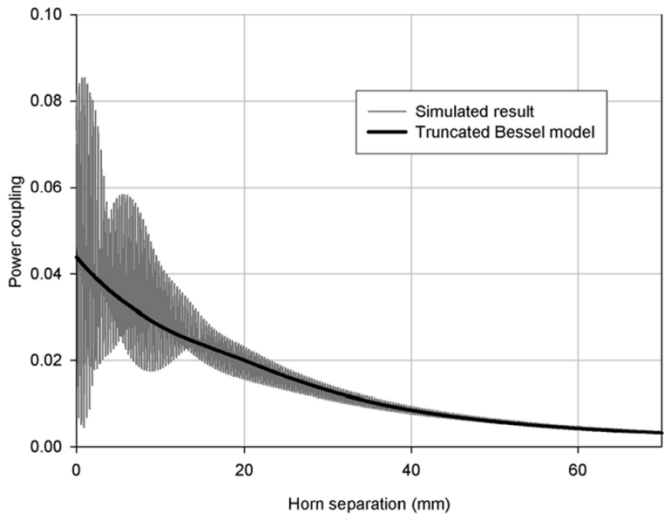

Fig. 10. Power coupling of a simple truncated Bessel model of the corrugated horns (thick line) compared to model prediction calculated over a 70 mm range.

IV. Conclusion

In this paper, we have presented a technique for calculating power coupling between two horns including the total transmission and reflection properties of an entire optical system, with a full electromagnetic description of the corrugated horns involved. By extending the waveguide modal-matching technique, to describe freespace propagation, this allows multiple reflections or standing waves to be predicted in simple optical systems. We have applied this theory to analyze the interesting effects observed when two corrugated horns are placed close together in transmitting and receiving mode. High Q cavity effects are observed when the horns are close together, especially when the horn fields are not well matched by an optical system. These effects have important consequences for heterodyne receivers of course where the LO horn is usually imaged to the detector horn via an optical system.

Further development of the approach is possible to understand the effects of placing real optical components between the horns. This opens up the possibility of designs with lossy apertures, for example, to reduce these standing wave effects.

Acknowledgment

The authors would like to thank the reviewers for their useful comments.

References

[1] R. Padman and J. A. Murphy, "A scattering matrix formulation for Gaussian beam-mode analysis," in *Proc. Inst. Elect. Eng. 7th Int. Conf. Antennas and Propagation (ICAP'91)*, Apr. 1991, pp. 201–204.

[2] A. D. Olver, P. J. B. Clarricoats, A. A. Kishk, and L. Shafai, *Microwave Horns and Feeds*. Piscataway, NJ: IEEE Press, 1994.
[3] P. Goldsmith, *Quasioptical Systems: Gaussian Beam Quasioptical Propagation and Applications*. Piscataway, NJ: IEEE Press, 1998, p. 17.
[4] J. A. Murphy, N. Trappe, and S. Withington, "Gaussian beam mode analysis of partial reflections in simple quasioptical system fed by horn antennas," *Infrared Phys. Technol.*, to be published.
[5] J. A. Murphy, A. Egan, and S. Withington, "Truncation efficiency in beam waveguides using Gaussian beam mode analysis," *IEEE Trans. Antennas Propag.*, vol. 41, no. 10, pp. 1408–1413, Oct. 1993.
[6] D. Martin and J. Bowen, "Long wave optics," *IEEE Trans. Microwave Theory Tech.*, vol. 41, no. 10, pp. 1676–1689, Oct. 1993.
[7] R. J. Wylde, "Millimeter wave Gaussian beam mode optics and corrugated feed horns," *IEEE Proc.*, vol. 131, pp. 158–262, 1984.
[8] J. A. Murphy, M. McCabe, and S. Withington, "Gaussian beam mode analysis of the coupling of power between horn antennas," *Int. J. Inf. Mill. Waves*, vol. 18, pp. 501–507, 1997.
[9] W. Jellema, S. J. Wijnholds, P. R. Wesselius, S. Withington, G. Yassin, J. A. Murphy, C. O'Sullivan, N. Trappe, T. Peacocke, and B. Leone, "Performance characterization and measurement results of a submillimeter-wave near-field facility for the heterodyne instrument for the far-infrared," presented at the *Proc. 3rd ESA Workshop Millimetre Wave Technology and Applications*, Espoo, Finland, May 2003.

Neil Trappe received the B.Sc. degree in applied physics from the University of Limerick, Limerick, Ireland, in 1998 and the Ph.D. degree in long wavelength optical analysis techniques from the Experimental Physics Department from the National University of Ireland, Maynooth, in January 2002.

He was a Postdoctoral Research Associate in long wavelength optical analysis techniques in the Experimental Physics Department at the National University of Ireland, until June 2003. Currently he is employed as a Lecturer in the Experimental Physics Department at the same university. His research interests are in the field of far-infrared space optics.

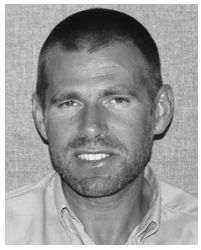

J. Anthony Murphy (M'88) received the B.Sc. and M.Sc. degrees in experimental physics from the University College Cork, Corek, Ireland, in 1977, the M.S. degree in physics from the California Institute of Technology, Pasadena, in 1981, and the Ph.D. degree from Cambridge University, Cambridge, U.K., in 1986.

He currently holds the position of Professor of Experimental Physics and Head of Department at the National University of Ireland, Maynooth. His main research area is in terahertz optics.

Stafford Withington (M'89) is a University Reader in Infrared and Millimeter-wave Physics in the Astrophysics Group, Cavendish Laboratory, University of Cambridge, Cambridge, U.K. His main area of interest is in the submillimeter-wave band, where he develops optics, detectors, and low-noise instrumentation for astronomy.

Dr. Withington is a Fellow of Downing College, Cambridge, U.K.

Willem Jellema was born in Bedum, Groningen, The Netherlands, on December 5, 1974. He received the Masters degree (*cum laude*) in applied physics from the Royal University of Groningen (RuG) in 1998. Currently, he is working toward the Ph.D. degree in physics at SRON in a scientific collaboration with the University of Cambridge and the Kapteyn Astronomical Institute, Groningen.

In 1998, he became Instrument Scientist for the National Institute for Space Research of the Netherlands (SRON). His research interests are in developing experimental techniques for submillimeter-wave optical systems and modeling of long-wave optics.